

Piezo-mechanical impedance of nanosized CdS single crystal

A.B. Bogoslovskaya¹, O.M. Khalimovskyy², D.O. Grynko¹

¹*V. Lashkaryov Institute of Semiconductor Physics, NAS of Ukraine,
41, prospect Nauky, 03680 Kyiv, Ukraine,
E-mail: dgrynko@gmail.com*

²*National Technical University of Ukraine "Igor Sikorsky Kyiv Polytechnic Institute"
37, prospect Peremohy, 03056 Kyiv, Ukraine*

Abstract. The design of a piezo-mechanical device based on nanosized CdS single crystal is a challenging task for demonstration of both the technological capabilities of crystal growth control in order to form simple sensor device topologies and the integrated usage of unique material properties with bottom-up approach. Analysis of luminescence spectra of CdS nanocrystals grown from the gas phase at the temperature 400 °C in the quasi-closed volume revealed that doping takes place with tin, as a component of ITO conductive film, simultaneously with doping with gold or silver from catalyze droplets. Piezo-mechanical longitudinal vibrations along the main symmetry axis of wurtzite-type single crystal have been presented in the continuous medium approximation based on experimental values of the nanocrystal piezo-module. Theoretical analysis of the frequency dependence of resonance oscillations for the nanosized beam-type piezo-mechanical resonators based on the CdS nanocrystal enabled to ascertain the equivalent RLC two-pole and values of the equivalent elements L and C prognosticated: there are high values of L – tens and hundreds of henry and very small values of the series capacitance of the order of femto- and attofarads. Below the resonance, the impedance of the crystal reaches gigaohms and has an inductive character.

Keywords: nanocrystal, nanowire, photoluminescence, piezoeffect, nano-electro-mechanical device.

<https://doi.org/10.15407/spqeo22.04.479>
PACS 77.65.-j, 78.67.Bf, 78.67.Uh

Manuscript received 26.08.19; revised version received 23.09.19; accepted for publication 29.10.19; published online 08.11.19.

1. Introduction

Luminescence, photoconductivity, and piezoelectricity of cadmium sulfide crystals attracted attention of numerous researchers in 1960–1980 ys. And even though photochemical reactions between non-equilibrium charge carriers and defects in CdS crystal can lead to some irreproducibility of material properties [1], the same mechanisms underlie photo-plastic and electro-plastic effects, nonlinear interaction with intense laser radiation and other promising effects. The complex of these material properties is clearly manifested in CdS nano- and micro-sized single crystals, complemented with a number of size effects, which expands the possibilities to design new electronic, opto-electronic and electro-mechanical nanodevices. A wide list of semiconductive nanocrystals, their shape- and size-specific properties and growth processes are basic object features for creation of micro- and nanoscaled devices and underlie the down-up approach, which was manifested by [2] and developed by numerous followers [3].

The design of a piezo-mechanical device based on a single crystal of nanosized CdS is a promising task to demonstrate both the technological capabilities of crystal growth control in order to form simple workable device topologies and the integrated usage of unique material properties. We are working on the usage of features of nanocrystals growth processes that allow formation of filamentary-like and more complex topologies of nanoobjects by using guided self-organization effects sometimes are easier than the traditional techniques of planar technology [4-6]. Earlier, we demonstrated several new techniques for CdS crystals growth [7-9] that allow controlling morphology, size, position on the substrate and the crystal structure of CdS nanosized crystals during chemical condensation from the gas phase in a quasi-closed volume. These techniques allow to grow CdS single crystals with a characteristic diameter of 20 up to 500 nm, length of 100 nm up to 1 mm, of both wurtzite and zinc-blende type of crystal symmetry.

Heteroepitaxial growth of CdS nanocrystal is a powerful tool to control its morphology. In the case of heteroepitaxy, the crystallographic structure of semiconductor substrates governs the orientation of grown nanocrystal. As a result, CdS single crystal structure with firmly fixed crystal diameter and orientation has been grown on Si substrate [9].

Nanocrystal growth region allocates on the crystal tip at vapour-solid [7], vapour-liquid-solid [7] or heteroepitaxial growth in contrary to micro-crucible mechanism for CdS growth on the surface of pyrolytic carbon microfiber, while the reaction zone is located on the base of the nanocrystal [8, 10].

Knowledge of diffusion length, nucleation time and crystallization rate as a function of conditions of growth allows us to control crystallinity and morphology of nanocrystals and fabricate bulk heterojunction structures for solar cell applications [10, 11].

Investigation and simulation of the piezo-mechanical and piezo-electric properties of micro- and nanosized single crystals is necessary for the development of optimal methods in the usage of nanocrystals morphology and vibration modes for an optimal structure of nanodevices. The mechanical resonance of a piezoelectric single CdS nanocrystal was observed by the authors [12]. The nanocrystal was fixed in the inter-electrode gap by a complex combined technique: growing an array of gas-phase wurtzite nanocrystals with a gold catalyst, obtaining a nanocrystal emulsion by ultrasonic treatment, capillar-oriented deposition onto electrodes and fixing with junctions formation by electron-beam lithography on an individual object, plasma etching and deposition of Ti/Au. The mechanical vibrations of the nanocrystal were recorded by an optical interferometric method, but current-voltage output was not measured. Piezo-phototronic effect enhanced responsivity and influence of piezo-effect on the junction properties of nanosized CdS_xSe_{1-x} single crystal was investigated experimentally and explained theoretically for frequency scale much below piezo-resonance [13].

Piezo-response of CdS nanocrystals depends on the crystal symmetry type significantly. CdS single crystals can have both a wurtzite or zinc-blende symmetry type. The difference in the symmetry of the crystal lattices leads to a difference in the piezomechanical tensors d_{ij} or e_{ij} symmetry, the general form of which is well known [14] and represented by matrices for wurtzite (1) and zinc-blende (2), respectively, in the principal axes:

$$d^{WZ}[0001] = \begin{pmatrix} 0 & 0 & 0 & 0 & d_{15} & 0 \\ 0 & 0 & 0 & d_{15} & 0 & 0 \\ d_{31} & d_{31} & d_{32} & 0 & 0 & 0 \end{pmatrix}, \quad (1)$$

$$d^{ZB}[001] = \begin{pmatrix} 0 & 0 & 0 & d_{14} & 0 & 0 \\ 0 & 0 & 0 & 0 & d_{14} & 0 \\ 0 & 0 & 0 & 0 & 0 & d_{14} \end{pmatrix}. \quad (2)$$

The preferable direction of zinc-blende crystal growth is [111] direction. Piezo-responses of zinc-blende with [111] direction differ from those of wurtzite with [0001] axis (3):

$$d^{ZB}[111] = \begin{pmatrix} d_{11} & -d_{11} & 0 & 0 & d_{15} & 0 \\ 0 & 0 & 0 & d_{15} & 0 & d_{26} \\ d_{31} & d_{31} & d_{32} & 0 & 0 & 0 \end{pmatrix}. \quad (3)$$

The wurtzite-type single crystal has a piezo-response to deformation of longitudinal compression-stretching, transverse compression-stretching and shear. A single crystal of zinc-blende symmetry with [001] direction gives a piezo-response onto shear strain and has no piezo-response to longitudinal compression-stretching.

Dislocations and linear defects of real nanosized single crystal can act [15] on the value of some matrix elements. Apparently, the values of the matrix elements of the piezo-electric tensor can be determined experimentally by measuring the piezoelectric response of individual nanocrystals, with KPFM technique [16], for example, as well as studying the piezo-mechanical resonances impedance with various excitation methods. This way requires to construct the model for comparison with experiment and predicting the properties of nanodevices.

This paper is devoted to analyzing the most simple task – piezo-mechanical longitudinal vibrations along the main symmetry axis of wurtzite-type single crystal in the continuous medium approximation.

2. Techniques

In our experiments, nanocrystals were grown from the gas phase in a quasi-closed volume. The extended control of nanocrystals growth from the gas phase gave us the possibility to change their morphology from amorphous or polycrystalline nanowires to single crystal nanoobjects. For piezo-response measurements, near-vertically aligned pattern of single crystals with close height and diameter values within the range 200 to 500 nm and interspace 500...1000 nm [6] was used. Magnetron-sputtered ITO with the resistance above 300 Ohm/sq and mean roughness up to 0.5 nm on the molybdenum glass were used as substrates for growing the CdS crystals. Ag or Au thin films with mean mass thickness 0.5 to 2.5 nm (controlled with 8 MHz quartz microbalance) were deposited using thermal evaporation and condensation in vacuum and were used to catalyze the CdS nanocrystal growth after annealing at 400...620 °C in vacuum. The conductivity of ITO dropped to 1500...9000 Ohm/sq after thermal and chemical treatment during the CdS crystals growth.

The photoluminescence of an array of nanocrystals was studied to confirm the fact of various doping of nanocrystals. Luminescence was measured with the samples grown under the same conditions of transport

and vapor supersaturation as the samples for measuring the piezoelectric effect, but with a long growth time of 5...25 min. Photoluminescence was studied at room temperature with the LabRamHR800 using the He-Cd laser with the excitation wavelength 325 nm.

Piezoelectric properties of each CdS nanosized single crystal in the grown array were measured with KPFM technique (MFP-3D AFM AsylumResearch) below the crystal resonance [6]. Silicon tips with nominal radius 100 nm and diamond-N cover were used for nanocrystals morphology and piezo-response measurements.

Piezo-mechanical longitudinal vibrations along the main symmetry axis of wurtzite-type single crystal were analyzed in the continuous medium approximation [14]. Numerical calculations were realized with the MathCAD software and using the set of well-known measured material values.

3. Photoluminescence and piezo-response of CdS nanosized crystals

The components d_{33} and d_{15} of piezoelectric matrix for single crystal were measured for near-vertically aligned nanocrystals [6]. Facets of vertically aligned CdS crystals in the grown array with SEM image like to the six-fold prism and their crystal type may be interpreted as those of the wurtzite structure. With assumption of wurtzite-type crystal symmetry, the results of piezo-response measurements may be interpreted for components of the matrix (1). In the case of non-longitudinal excitation of a wurtzite-type single crystal or an experiment with zincblende crystal, the interpretation of the measured piezoelectric response will be different, *i.e.*, we have encountered with the model-related result.

Results of calculation of piezoelectric modules in wurtzite-type symmetry crystal [6] for CdS nanocrystals, grown on ITO without usage of Au or Ag catalysts, are $d_{33} = 15$ pm/V and $d_{15} = 0.5$ pm/V. The piezomodule d_{33} is 1.6 pm/V for Au catalyst and ITO layer. In the case of Ag catalyst and ITO layer d_{33} is 3.6 pm/V.

Since dispersion of piezo-responses for a few kinds of CdS nanosized crystals is within one order, then we have associated their values with impact of doping. Luminescence spectra of CdS nanosized crystals express crystal defects, doping and surface states quite reliably [17, 18]. Normalized luminescence spectra of CdS nanosized crystals pattern are presented in Fig. 1.

All types of CdS crystals are characterized by the presence of their own narrow band with a maximum of about 510 nm and wide impurity bands. The impurity bands for CdS crystals grown with the Au catalyst differ significantly depending on whether the crystals were grown with or without an additional ITO layer. Significant change in the conductivity of the ITO layer after crystal growth indicates a partial decomposition of ITO at the temperature 400...600 °C with a pure phase of Sn separation. A significant difference in the luminescence spectra 3 and 4 (Fig. 1) and the fact that

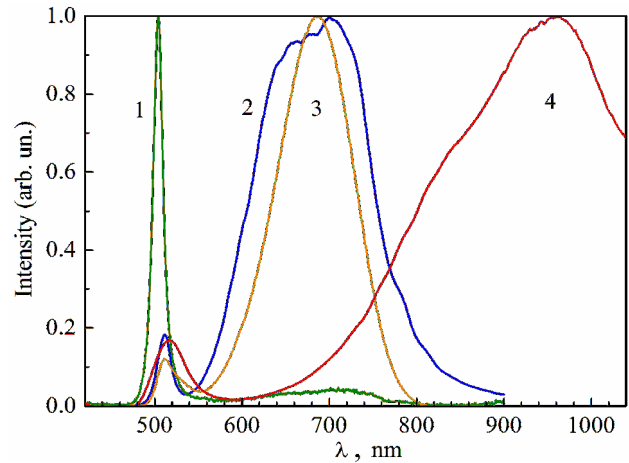


Fig. 1. Normalized spectra of luminescence of CdS nanocrystals grown using the vapor-solid method on glass (1) and the vapor-liquid-solid method with Ag, as nucleus, on ITO (2) and with Au nucleus on glass substrate (3) and on ITO film (4).

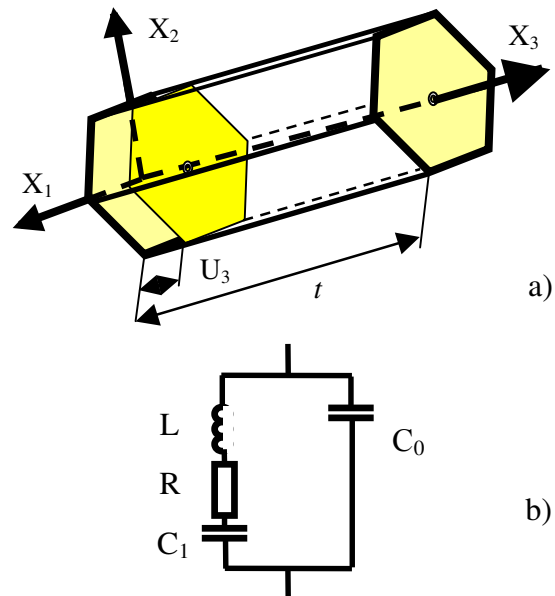


Fig. 2. Coordinate system for the problem of longitudinal piezo-mechanical vibrations of a hexagonal symmetry crystal (a) and equivalent two-pole circuit for a piezo-mechanical resonator, based on CdS nanosized crystal (b).

a significant change in the conductivity of the ITO layer after crystal growth indicates the doping of CdS crystals with not only Au but with Sn as well.

Similar difference in luminescence was registered for the silver catalyst grown over ITO layer. Doping CdS with Au may be quite different as compared to doping with the pair Au and Sn. We may assume defects coupling in the volume or at the surface of nanocrystals, which may explain luminescence spectra difference. Doping may produce polarizable defects that are able to appear in the luminescence and piezo-response of nanocrystal.

4. Formulation of the problem

In accord with [14, 19, 20], let's write the relation between pressure and deformation for a semi-infinite piezoelectric crystal with an axis of symmetry oriented along the coordinate X_3 in the axes of the coordinates depicted in Fig. 2a in the units of CGSE system:

$$\begin{aligned} T_3 &= C_{33}^E \cdot S_3 - e_{33} \cdot E_3, \\ D_3 &= \epsilon_{33}^S \cdot E_3 + e_{33} \cdot S_3 \end{aligned} \quad (4)$$

and boundary conditions on the side surfaces of the crystal perpendicular to the X_3 axis:

$$\frac{\partial D_3}{\partial x_3} = 0, \quad (5)$$

where F_i is the force, u_i – shift of crystal zone, T_i – pressure, S_i – deformation, C_{ij}^E – stiffness coefficient at the constant electric field, E_i – electric field, D_i – electric-flux density, ϵ_{ij}^S – dielectric susceptibility at constant deformation, e_{ij} – piezoelectric coefficient of the crystal, ω – frequency, ρ – density, t – length of crystal along the symmetry axis, S_a – electrical contact area.

Relations with external circuits through the equation are: $F_3 = T_3 \cdot S_a$ force on the sides of the crystal at $X_3 = 0$, t and current at $X_3 = 0$, t

$$I = j \cdot \omega \cdot D_3 \cdot S_a. \quad (6)$$

The potential difference between the side faces of the crystal is

$$V = \int_0^t E_3 \cdot dx_3. \quad (7)$$

From the pair of equations (4), taking into account the equations of dynamics of the material point, one can obtain the equations for piezo-mechanical motion of the crystal elements:

$$\begin{aligned} \rho \frac{\partial^2 u_3}{\partial t^2} &= \frac{\partial T_3}{\partial x_3} = \frac{\partial}{\partial x_3} \left[\frac{C_{33}^E \cdot S_3 - e_{33} \cdot (D_3 - e_{33} \cdot S_3)}{\epsilon_{33}^S} \right] = \\ &= \left(C_{33}^E + \frac{e_{33}^2}{\epsilon_{33}^S} \right) \cdot \frac{\partial^2 u_3}{\partial x_3^2}. \end{aligned} \quad (8)$$

5. An equivalent electrical circuit

An equivalent electric circuit of a piezo-mechanic resonator is important for modeling the linear properties of a device in different resonator geometries.

Eq. (8) describes the current and potential in an electric four-pole circuit compiled of resistors, capacitances, inductances, and transformers. The structure of this four-pole and the value of the elements are defined on the basis of equation (8). The rather

complicated structure of the four-pole, which directly corresponds to (8), can be simplified [19] using the methods of equivalent transformations of radio-engineering circuits into the simplest two-terminal one (Fig. 2b). Below, one sees the expressions for the elements of the equivalent scheme of the piezo-mechanical resonator in the system of ISQ units, which were calculated on the basis of Eqs. (4):

- the equivalent capacitance of the crystal formed by the electrodes:

$$C_0 = \epsilon_{33}^S \cdot \epsilon_0 \cdot \frac{S_a}{t}, \quad (9)$$

- equivalent inductance:

$$L = \frac{\rho \cdot t^3}{8 S_a e_{33}^2} \quad (10)$$

- and piezo-mechanical series equivalent capacitance:

$$C_1 = \frac{C' \cdot (-C_0)}{C' - C_0},$$

$$\text{where } C' = \frac{8 \cdot S \cdot e_{33}^2}{\pi^2} \cdot t \cdot \left(C_{33}^E + \frac{e_{33}^2}{\epsilon_0 \cdot \epsilon_{33}^S} \right).$$

The ratio of capacitances is a function of the material constants of the substance, it is roughly

$$\frac{C_1}{C_0} = \frac{32 e_{33}^2}{\pi \cdot \epsilon_{33}^S \cdot C_{33}^E}. \quad (11)$$

The mechanical resonance frequency [12] is

$$F_{m0} = 0.8066 \sqrt{\left(C_{33}^E / \rho \right) \cdot (D/t^2)}, \quad (12)$$

where D is the crystal diameter.

The piezoelectric series-resonant frequency is independent of the crystal diameter

$$F_0 = \sqrt{\frac{C_{33}^E / \rho}{2t}}. \quad (13)$$

Losses are not directly determined from Eqs. (4), since any specific mechanism of losses was not introduced into the model.

For CdS, the material constants are well known: $C_{33}^E = 62 \cdot 10^{10} \text{ din/cm}^2$ [12], $e_{33} = d_{33} \cdot E = 1.2 \text{ K/m}^2$, where E is the intensity of external electric field applied to the crystal, dielectric susceptibility varies with the frequency, we used $\epsilon = 5$ [1]. Figs. 3 to 5 show the dependence of components of the equivalent scheme on the nanocrystal sizes.

The capacitances of the mounting wires and electrodes will be added to the capacitance C_0 .

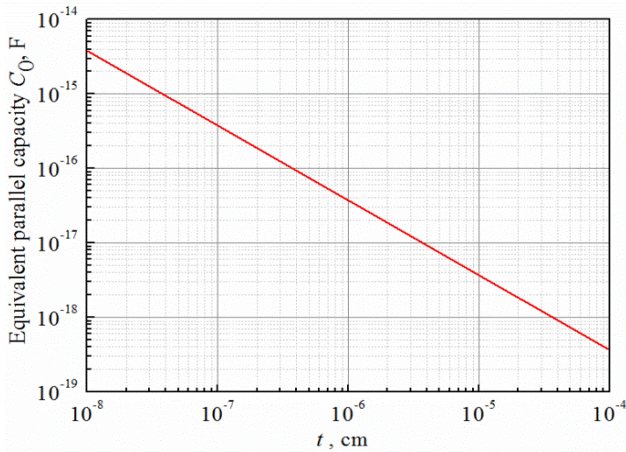


Fig. 3. The equivalent parallel capacitance C_0 of crystal CdS depending on the crystal length t with the diameter 100 nm.

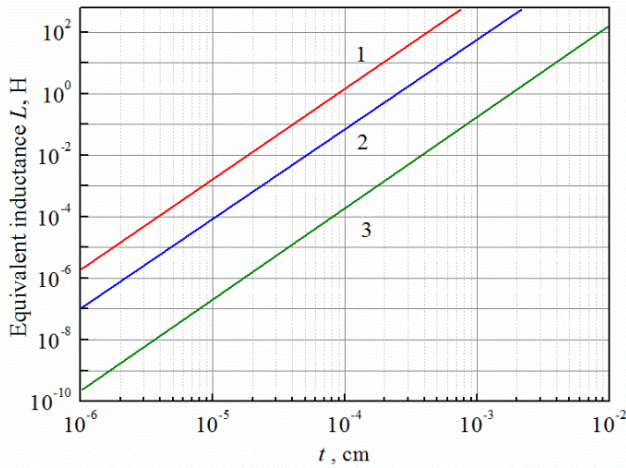


Fig. 4. The equivalent inductance L of a piezoresonator for CdS nanocrystals with the diameters 100 nm (1), 500 nm (2) and 10 μ m (3) depending on the length of the crystal t .

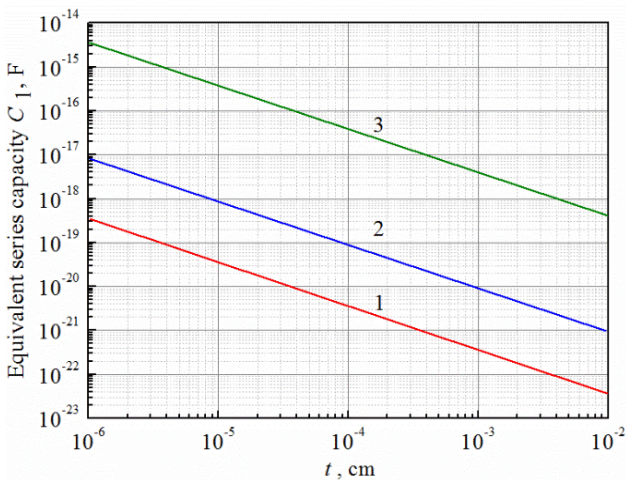


Fig. 5. The equivalent series capacitance C_1 of CdS nanocrystal, depending on the crystal length t for the diameters 100 (1), 500 (2) and 10000 nm (3).

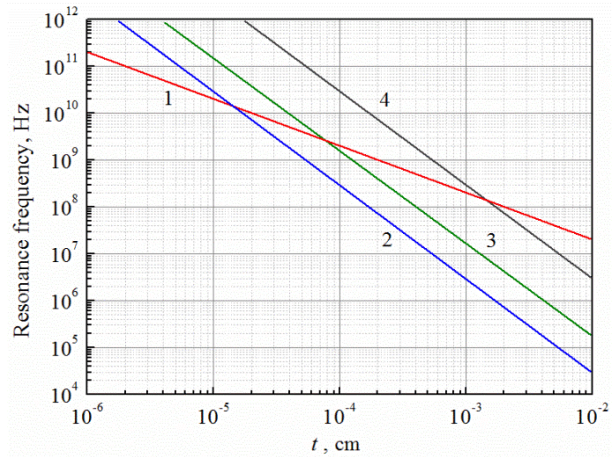


Fig. 6. Frequencies of series piezoelectric F_0 (1) and mechanical F_{m0} (2–4) resonances, depending on the crystal length t of the CdS crystal and different crystal diameters of 100 nm (2), 500 nm (3) and 10 μ m (4).

6. Impedance of CdS nanocrystal

The value of components in the equivalent scheme of a piezo-mechanical resonator is a unique function of the relation between the material constants CdS, geometry and sizes of the nanocrystal. The impedance of this circuit has its own peculiarities that need to be analyzed for the effective construction of measuring circuits.

The frequencies of the series piezoelectric F_0 and mechanical F_{m0} resonances, in dependence on the crystal size t , are presented in Fig. 6.

For a typical geometry of a nanocrystal, when the length significantly exceeds the diameter, the frequency of the mechanical resonance will be much lower than the piezoelectric frequency. This is due to the ratio of capacitances $(C_1/C_0) = 1.03 \cdot 10^{-2}$ for CdS. That is, these CdS resonator crystals are ineffective, since phase-shifting quartz resonators are made with special geometry. The close arrangement of the frequencies of the series piezoelectric F_0 and mechanical F_{m0} resonances is possible only in specimens of special geometry – in crystals with a ratio of diameter to length: $(D/t) = 0.62$.

In the frequency range below series resonance, the impedance of the resonator is inductive with a very high value of the $10^9 \dots 10^{13}$ Ohm module. The capacitance of electrodes, to which the nanocrystal are fixed, and the geometric capacitance C_0 of the crystal can shunt resonance behavior of the LC_1 circuit. Resonance behavior of a nanocrystal in the impedance measurement mode is very problematic, since the relative change in the impedance of the circuit is shunted by the input capacitance of the measuring device. Consequently, it is necessary to develop such methods for investigating the properties of a nanocrystal that do not depend on the capacitance of the input circuits of the measuring device.

7. Conclusions

A significant difference in the luminescence spectra and the fact of a significant change in the conductivity of the ITO layer after crystal growth indicate doping the CdS crystals with not only Au or Ag catalysts but with Sn as well. Piezoresponse for vertically aligned CdS nanocrystal is few times larger for CdS crystals doped with Sn than for doped with Ag or Au and Sn. Interpretation of piezoresponce is model-related, and in the cause of wurtzite-type crystal d_{33} is in the span 0.5–15 pm/V.

A theoretical analysis of frequency dependence of the resonance oscillations of the beam type piezo-mechanical resonator with CdS nanocrystal has been presented. The CdS nanocrystal is equivalent to the two-pole RLC, and values of the equivalent elements L , series and parallel capacitances C_1 and C_0 have been calculated using the experimental values of the module of the piezoelectric effect. The nanocrystals fixed by two electrodes are characterized by very high values of L – tens and hundreds of henry, and by very small values of the series capacitance within the orders of femto- and attofarads.

The frequencies of mechanical and series piezoelectric resonances are close only for crystals with a defined form factor: in the case of a cylinder-like geometry $(D/t) = 0.62$. Before series piezoelectric resonance, the impedance of the crystal reaches gigaohms and has an inductive character in the scale of megahertz. Thus, the CdS nanocrystal is not a two-pole with a large variation of the phase characteristic, which is similar to a quartz resonator. The influence of shunt capacitance of the input of measuring macrodevices on the possibility of direct measurements of the frequency response of nanocrystal is important.

References

- Georgobiani A.N., Sheynkman M.K. (eds.). *The Physics of A^{II}B^{VI} Compounds*. Moscow, Nauka, 1986 (in Russian).
- Lieber Ch.M. Nanoscale science and technology: Building a big future from small things. *MRS Bulletin*. 2003. **28**, No 7. P. 486–491. <https://doi.org/10.1557/mrs2003.144>.
- Zhang A., Zheng G., Lieber C. *Nanowires. Building Blocks for Nanoscience and Nanotechnology*. Springer, Switzerland, 2016. <https://doi.org/10.1007/978-3-319-41981-7>.
- Zubarev R.A., Solokha V.P., Galaktionov D.A., Rachkov A.E., Fedoryak A.N., Grynko D.A. Single crystal biosensor technology. *International Joint Workshop “Advanced process and device integration and innovative nanofunctions in Nanoelectronics”*, Kyiv, Ukraine, 2013. P. 87.
- Zubarev R.A., Solokha V.P., Galaktionov D.A., Rachkov A.E., Fedoryak A.N., Grynko D.A. Nanocrystals self-organizing as an approach for single crystal field-effect resistor preparation. *Workshop Nanostructures on two-dimensional solids (73 JUVSTA)*, Eisenerz, Austria, 2014. P. 66.
- Grynko D., Bortchagivsky E., Doroshenko T., Rachkov A., Styopkin V., Hesser G., Kratze M., Teichert C. Piezoelectric properties of self-organized nanosized single crystals of CdS and its prospects for piezoresonance sensors. *4th Annual Conference on Optical Nanospectroscopy*, Lisbon, Portugal, March 28-31, 2017.
- Grynko D.A., Fedoryak A.N., Dimitriev O.P., Lin A., Laghumavarapu R.B., Huffaker D.L. Growth of CdS nanowire crystals: Vapor–liquid–solid versus vapor–solid mechanisms. *Surface and Coatings Technology*. 2013. **230**. P. 234–238. <https://doi.org/10.1016/j.surfcoat.2013.06.058>.
- Smertenko P.S., Grynko D.A., Osipyonok N.M., Dimitriev O.P., Pud A.A. Carbon fiber as a flexible quasi-ohmic contact to cadmium sulfide micro- and nanocrystals. *phys. status solidi (a)*. 2013. **210**, No 9. P. 1851–1855. <https://doi.org/10.1002/pssa.201228805>.
- Grynko D.O., Fedoryak A.N., Dimitriev O.P., Kratzer M., Piryatinski Y.P. Template-assisted synthesis of CdS nanocrystal arrays in chemically inhomogeneous pores using a vapor-solid mechanism. *RSC Adv*. 2015. **5**, No 35. P. 27496–27501. <https://doi.org/10.1039/C5RA01175B>.
- Grynko D.A., Fedoryak O.M., Smertenko P.S., Dimitriev O.P., Ogurtsov N. A., Pud A.A. Hybrid solar cell on a carbon fiber. *Nanoscale Res. Lett*. 2016. **11**, No 1. P. 265–273. <https://doi.org/10.1186/s11671-016-1469-7>.
- Grynko D.A., Fedoryak O.M., Smertenko P.S., Ogurtsov N.A., Pud A.A., Noskov Yu.V., Dimitriev O.P. Application of CdS nanostructured layer in inverted solar cells. *J. Phys. D: Appl. Phys*. 2013. **46**. 495114 (10 pp.). <https://doi.org/10.1088/0022-3727/46/49/495114>.
- Kim Y.D., Heo K., Cho M.R., Cho S., Yoon D., Cheong H., Jian J., Hong S., Park Y.D. Determination of mechanical properties of single-crystal CdS nanowires from dynamic flexural measurements of nanowire mechanical resonators. *Appl. Phys. Exp*. 2011. **4**, No 6. P. 065004. <https://doi.org/10.1143/APEX.4.065004>.
- Guozhang Dai, Haiyang Zou, Xingfu Wang, Yuankai Zhou, Peihong Wang, Yong Ding, Yan Zhang, Junliang Yang, Zhong Lin Wang. Piezophototronic effect enhanced responsivity of photon sensor based on composition-tunable ternary CdS_xSe_{1-x} nanowires. *ACS Photonics*. 2017. **4**, No 10. P. 2495–2503. <https://doi.org/10.1021/acsp Photonics.7b00724>.

14. Burfoot J. C. *Ferroelectrics: An Introduction to the Physical Principles*. Van Nostrand, New York, 1967.
15. Kosevich A.M., Pastur L.A., Feldman E.P. Dislocation and linear charge fields in piezoelectric crystals. *Sov. Phys.-Crystallogr.* 1968. **12**, No 5. P. 797–801.
16. <https://www.asylumresearch.com/Applications/PFMAppNote/PFM-ANLR.pdf>
17. Bogoslovskaya A., Grynko D., Bortchagivsky E. Luminescent properties of CdS nanocrystals. *Topical meeting on Single Quantum Emitters (SQE 2017)*, Braga, Portugal, October 4-6, 2017.
18. Bogoslovskaya A.B., Grynko D.O., Bortchagovsky E.G., Gudymenko O.I. Luminescent analysis of the quality of CdS nanocrystals depending on technological parameters. *Semiconductor Physics, Quantum Electronics & Optoelectronics*. 2019. **22**, No 2. P. 231–236.
<https://doi.org/10.15407/spqeo22.02.231>.
19. Yakamichi Nakamoto, Toyosaka Moriizumi. A theory of a quartz crystal microbalance based upon a Mason equivalent circuit. *Jpn. J. Appl. Phys.* 1990. **29**, No 5. P. 963–969.
<https://doi.org/10.1143/JJAP.29.963>.
20. Brand O., Dufour I., Heinrich S., Josse F. *Resonant MEMS: Fundamentals, Implementation, and Application*. Wiley-VCH, France, 11. 2015.
<https://doi.org/10.1002/9783527676330>.

Authors and CV



Alla Bogoslovskaya, Senior scientific researcher at the Department of Physics of Optoelectronic devices, V. Lashkaryov Institute of Semiconductor Physics, NAS of Ukraine. The area of scientific interests includes: physics and technology of semiconductor nanostructured materials and device structures of optoelectronics; application of optical spectroscopy various techniques for semiconductive materials, structures and devices examination.



Oleksiy Khalimovskyy, Associate Professor at the Faculty of Electric Power Engineering and Automatics of National Technical University of Ukraine “Igor Sikorsky Kyiv Polytechnic Institute”. His research interests includes: pinpoint positioning actuators; precise control of electric drives coordinates for various mechanisms and applications; control of the production of polymer composite materials with specified structure; automatic control of feeding and its utilization for welding equipment.



Dmytro Grynko, Senior researcher at the Department of Functional Materials and Nanostructures (laboratory of the optoelectronic molecular-semiconducting systems) at the V. Lashkaryov Institute of Semiconductor Physics, NAS of Ukraine. Scope of research interests: functional molecular, low-dimensional nanostructures and nanocomposite nanostructured thin film media, gas-phase technology and application, template guided self-organization, technology of low-dimensional structures, nanowires, nanosized single crystals growth from gas-phase; gas-phase technology for multicomponent nanocomposites films based on fullerenes, organic dyes, organic polymers and non-organic compounds; CVD, organometallic compounds.